P-Type Gradient-Enhanced COSY Experiments Show Lower t_1 Noise than N-type

Timothy J. Horne and Gareth A. Morris*
Department of Chemistry, University of Manchester, Oxford Road, Manchester M13 9PL, UK

Many of the perturbations that lead to t_1 noise in 2D NMR spectroscopy cause fluctuations in the relative phases of pulses and coherences. Because the sensitivity of the phase of a coherence to changes in the phase of a pulse depends on the change of coherence order, P-type signals in homonuclear correlation experiments are insensitive to errors in the phase of the mixing pulse, and hence they show less t_1 noise than N-type signals. This effect is illustrated for the gradient COSY experiment. © 1997 John Wiley & Sons, Ltd.

Magn. Reson. Chem. **35**, 680–686 (1997) No. of Figures: 5 No. of Tables: 2 No. of References: 9

Keywords: NMR; COSY; gCOSY; gradient methods; t_1 noise

Received 13 March 1997; accepted 28 April 1997

INTRODUCTION

Since the first description of methods for obtaining information on the signs of f_1 frequencies in 2D correlation experiments, it has been recognized that there is a choice to be made between P-type (or anti-echo) coherence transfer pathways, in which the signs of precession frequencies in f_1 and f_2 are the same, and N-type (or echo) pathways, in which the signs are opposite. The first successful such experiment, homonuclear correlation using the SECSY sequence,[1] used the EXORCYCLE phase cycle to select the coherence transfer echo N-type pathway. The form of the SECSY experiment was dictated by the convenience of using the same software as 2D *J* spectroscopy, which requires N-type selection. Later, the same type of phase cycling was introduced into the COSY experiment,[2] giving the absolute value COSY experiment that is still widely used and is the parent of more recent gradient-enhanced methods.[3] With absolute value COSY there is essentially a free choice between the echo (N-type) and anti-echo (P-type) pathways, and the two are nowadays used virtually interchangeably.

In the original work on absolute value COSY,[2] it was argued that in most systems of interest the P-type pathway was preferable because it discriminated against the signals of solvent and of small molecule impurities, since these tend to have longer spin–spin relaxation times and hence have more to lose from static field inhomogeneity. Choosing the P-type pathway can thus lead to spectra which show slightly less interference from sharp unwanted signals. The same argument can, however, equally well be deployed in reverse: the N-type pathway refocuses the effects of field inhomogeneity, and hence gives more signal than the P-type. The relative merits of the two arguments are in practice rarely important; both pathways normally give good results. There is, however, a further argument in favour of the P-type pathway which is potentially significant: that where the coherence transfer pathway is selected by field gradient pulses, it reduces the susceptibility of the experiment to instrumental irreproducibility, and hence can give spectra with less t_1 noise. The most effective way to reduce t_1 noise is by the use of reference deconvolution[4] to correct the phases, amplitudes, frequencies and lineshapes of the signals measured in heteronuclear[5] or homonuclear[6] 2D experiments. This technique can give signal to t_1 noise ratios in excess of 100 000:1, more than an order of magnitude better than is commonly obtained with modern instruments, but is not yet widely available.

THEORY

Consider the effect of changes in pulse phase on the signals seen in a generic COSY experiment. For the purposes of this analysis it does not matter whether the signal of interest comes from a diagonal peak or a cross peak; for simplicity it may be assumed to be a diagonal peak singlet. Let the receiver reference phase be arbitrarily fixed as zero, and let the phases of the two pulses of a COSY experiment be ε_1 for the initial pulse and $\phi + \varepsilon_2$ for the mixing pulse, where ϕ is an arbitrary phase shift (which in practice will normally be a multiple of 90°) and ε_1 and ε_2 are small phase errors. Figure 1 shows in schematic form a general pulse sequence which may be used for phase-cycled, P-type gradient enhanced or N-type gradient-enhanced absolute value COSY, depending on the magnitudes and signs of the field gradient pulses used. The field gradient pulses are assumed to be of equal duration τ and magnitude G_z, and either of the same sign (for N-type pathway selection) or of

* *Correspondence to*: G. A. Morris. Email: g.a.morris@man.ac.uk.
Contract grant sponsor: EPSRC; *Contract grant number*: GR/H59251; *Contract grant number*: GR/K16296.

 CCC 0749–1581/97/100680–07 $17.50

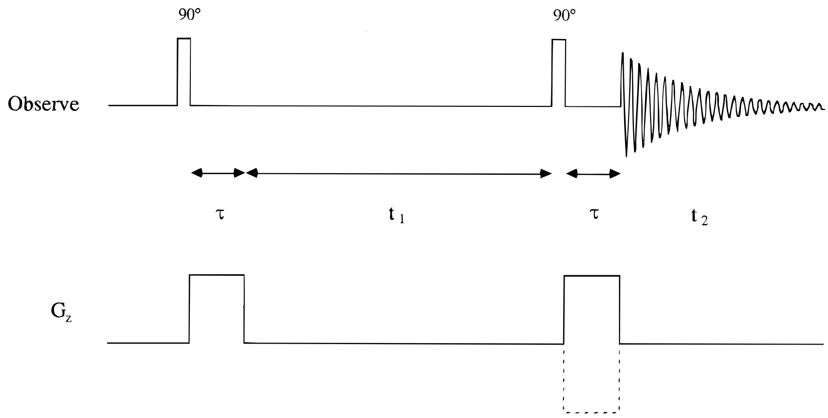

Figure 1. Generic pulse sequence for absolute value COSY with f_1 quadrature detection. The field gradient pulses are of zero amplitude and duration in phase-cycled COSY, of equal magnitude and the same sign in P-type gCOSY and of equal magnitude and opposite sign in N-type gCOSY.

opposite sign (for P-type). If a spin I is initially at equilibrium in state I_z, then the signal recorded at some time t_2 during acquisition may be written in the form $M_{xy} = M_y - iM_x$, where M_y is the coefficient of I_y in the state of I at the end of the pulse sequence and M_x is the coefficient of I_x. If the offset from resonance of spin I is ω, then the angles through which resonance offset causes I to precess during the times $t_1 + \tau$ and $t_2 + \tau$ are $\theta_1 = \omega(t_1 + \tau)$ and $\theta_2 = \omega(t_2 + \tau)$, respectively. The effects of the two field gradient pulses at the start of t_1 and of t_2 will depend on the position z of spins in the sample; if $\theta_z = \gamma G_z z\tau$ then the two precession angles θ_{z1} and θ_{z2} resulting from precession during the two field gradient pulses will be θ_z and $\pm\theta_z$, respectively.

Neglecting relaxation, after the first pulse the state of the system can be represented as

$$\sigma^1 = I_x \sin \varepsilon_1 - I_y \cos \varepsilon_1 \quad (1)$$

and at the end of the evolution period

$$\sigma^2 = I_x \sin(\varepsilon_1 + \theta_1 + \theta_{z1}) - I_y \cos(\varepsilon_1 + \theta_1 + \theta_{z1}) \quad (2)$$

If the mixing pulse is of flip angle 90°, then it will purge all components of σ^2 that are not in phase with it, giving

$$\begin{aligned}\sigma^3 = {} & I_x \cos(\phi + \varepsilon_2) \sin(\varepsilon_1 + \theta_1 + \theta_{z1} - \phi - \varepsilon_2) \\ & + I_y \sin(\phi + \varepsilon_2) \sin(\varepsilon_1 + \theta_1 + \theta_{z1} - \phi - \varepsilon_2) \\ & - I_z \cos(\varepsilon_1 + \theta_1 + \theta_{z1} - \phi - \varepsilon_2) \quad (3)\end{aligned}$$

so that at time t_2 the signal measured will be proportional to

$$\begin{aligned}M_{xy}(t_1 t_2) = {} & -i \exp[i(\phi + \varepsilon_2 + \theta_2 + \theta_{z2})] \\ & \times \sin(\theta_1 + \theta_{z1} + \varepsilon_1 - \varepsilon_2 - \phi) \quad (4)\end{aligned}$$

where the final term θ_{z2} in the exponential will be positive if the field gradient pulse at the start of the detection period has a positive sign (N-type selection), and negative if the gradient pulse is negative (P-type selection).

For P-type and N-type gCOSY, the phase ϕ of the mixing pulse may be set to zero without loss of generality. Any terms in $M_{xy}(t_1, t_2)$ in which θ_{z1} is not cancelled by θ_{z2} will vary rapidly with position z, so that the integrated signal over the sample from such terms will be small and may be neglected; this is the basis of the coherence transfer pathway selection. The surviving terms for the P-type and N-type pathways respectively are

$$M^{\mathrm{P}}_{xy}(t_1, t_2) = -\frac{i}{2} \exp(i\varepsilon_1) \exp[i(\theta_1 + \theta_2)] \quad (5)$$

and

$$M^{\mathrm{N}}_{xy}(t_1, t_2) = -\frac{i}{2} \exp[i(2\varepsilon_2 - \varepsilon_1)] \exp[i(\theta_1 + \theta_2)] \quad (6)$$

in which, as expected, both signals are phase modulated by ω_1 and ω_2 and shifted by the phase error in the first pulse ε_1, but only the N-type pathway is affected by any phase error ε_2 in the mixing pulse.

The analysis of the N- and P-type phase cycled absolute value COSY experiments is sightly more complex because in general each phase error will be different in each of four transients measured with different mixing pulse phases, and each of the four measured free induction decays has to be phase shifted appropriately before co-addition. However, no field gradient pulses are used, so the angles θ_{z1} and θ_{z2} are zero. Keeping the phase of the initial pulse set to nominal zero (except for a small error ε_1), if the mixing pulse phase ϕ is set to 0°, 90°, 180° and 270° in successive transients then keeping the receiver phase constant will select the P-type pathway, and using receiver phases of 0°, 180°, 0°, 180° will select the N-type. If the phase errors of the two pulses in the four transients are ${\varepsilon_1}^1$ to ${\varepsilon_1}^4$ and ${\varepsilon_2}^1$ to ${\varepsilon_2}^4$, respectively, then the results of adding together the appropriately phase shifted signals for the two versions of the phase cycle will be

$$\begin{aligned}M^{\mathrm{P}}_{xy}(t_1, t_2) = {} & -i \exp(i\theta_2)\{\exp(i{\varepsilon_2}^1) \\ & \times [\sin\theta_1 + \cos\theta_1 \sin({\varepsilon_1}^1 - {\varepsilon_2}^1)] \\ & -i \exp(i{\varepsilon_2}^2)[\cos\theta_1 - \sin\theta_1 \sin({\varepsilon_1}^2 - {\varepsilon_2}^2)] \\ & +\exp(i{\varepsilon_2}^3)[\sin\theta_1 + \cos\theta_1 \sin({\varepsilon_1}^3 - {\varepsilon_2}^3)] \\ & -i \exp(i{\varepsilon_2}^4)[\cos\theta_1 - \sin\theta_1 \sin({\varepsilon_1}^4 - {\varepsilon_2}^4)]\} \quad (7)\end{aligned}$$

for the P-type pathway and

$$\begin{aligned} M_{xy}^{\mathrm{N}}(t_1, t_2) = -i\exp(i\theta_2)\{&\exp(i\varepsilon_2{}^1) \\ &\times [\sin\theta_1 + \cos\theta_1 \sin(\varepsilon_1{}^1 - \varepsilon_2{}^1)] \\ &+ i\exp(i\varepsilon_2{}^2)[\cos\theta_1 - \sin\theta_1 \sin(\varepsilon_1{}^2 - \varepsilon_2{}^2)] \\ &+ \exp(i\varepsilon_2{}^3)[\sin\theta_1 + \cos\theta_1 \sin(\varepsilon_1{}^3 - \varepsilon_2{}^3)] \\ &+ i\exp(i\varepsilon_2{}^4)[\cos\theta_1 - \sin\theta_1 \sin(\varepsilon_1{}^4 - \varepsilon_2{}^4)]\} \end{aligned} \quad (8)$$

for the N-type.

If the phase errors ε can be assumed to be small, then linear approximation may be used for their exponentials, giving the following expressions for the P- and N-type gCOSY signals:

$$M_{xy}^{\mathrm{P}}(t_1, t_2) = -\frac{i}{2}\exp[i(\theta_1 + \theta_2)](1 + i\varepsilon_1) \quad (9)$$

and

$$M_{xy}^{\mathrm{N}}(t_1, t_2) = -\frac{i}{2}\exp[i(\theta_1 + \theta_2)][1 + i(2\varepsilon_2 - \varepsilon_1)] \quad (10)$$

and for the P-type and N-type phase cycled COSY:

$$\begin{aligned} M_{xy}^{\mathrm{P}}(t_1, t_2) = -i\exp(i\theta_2)[&-2i\exp(i\theta_1) + i\sin(\theta_1) \\ &\times (\varepsilon_2{}^1 + \varepsilon_2{}^3 + \varepsilon_1{}^2 - \varepsilon_2{}^2 + \varepsilon_1{}^4 - \varepsilon_2{}^4) \\ &+ \cos\theta_1(\varepsilon_2{}^2 + \varepsilon_2{}^4 + \varepsilon_1{}^1 - \varepsilon_2{}^1 + \varepsilon_1{}^3 - \varepsilon_2{}^3)] \end{aligned} \quad (11)$$

$$\begin{aligned} M_{xy}^{\mathrm{N}}(t_1, t_2) = -i\exp(i\theta_2)[&-2i\exp(i\theta_1) + i\sin\theta_1 \\ &\times (\varepsilon_2{}^1 + \varepsilon_2{}^3 - \varepsilon_1{}^2 + \varepsilon_2{}^2 - \varepsilon_1{}^4 + \varepsilon_2{}^4) \\ &+ \cos\theta_1(\varepsilon_1{}^1 - \varepsilon_2{}^1 + \varepsilon_1{}^3 - \varepsilon_2{}^3 - \varepsilon_2{}^2 - \varepsilon_2{}^4)] \end{aligned} \quad (12)$$

The relative amounts of t_1 noise in each of the four experiments may now be calculated. According to Parseval's theorem, the integrated noise power in the f_1 dimension of the final 2D spectrum will be the same as that in the t_1 time domain, so the t_1 noise seen in an absolute value mode spectrum will be proportional to the square root of the sum of the squares of the error contributions. If the errors are all uncorrelated and of equal root mean square amplitude ε, then the ratios N/S of the root mean square error signal amplitudes to the moduli of the signals will be

$$(N/S)^{\mathrm{P}} = \varepsilon \quad (13)$$

and

$$(N/S)^{\mathrm{N}} = \sqrt{4\varepsilon^2 + \varepsilon^2} = \sqrt{5}\,\varepsilon \quad (14)$$

for the gCOSY experiments and

$$(N/S)^{\mathrm{P}} = \frac{\sqrt{6\varepsilon^2 \sin^2\theta_1 + 6\varepsilon^2 \cos^2\theta_1}}{2} = \sqrt{\frac{3}{2}}\,\varepsilon \quad (15)$$

and

$$(N/S)^{\mathrm{N}} = \frac{\sqrt{6\varepsilon^2 \sin^2\theta_1 + 6\varepsilon^2 \cos^2\theta_1}}{2} = \sqrt{\frac{3}{2}}\,\varepsilon \quad (16)$$

for the phase-cycled experiments. The effect of time averaging on t_1 noise will be to improve the ratio of signal to t_1 noise by $\sqrt{n}$, where n is the number of transients co-added, if the perturbations in successive transients are uncorrelated. Here the phase-cycled experiments were analysed for an experiment using four transients and the gradient-enhanced experiments using only one, so the relative amounts of t_1 noise expected for experiments using equal numbers of transients per increment will be halved for the gradient techniques. This gives a final ratio of $1:\sqrt{5}:\sqrt{6}$ (there is an unfortunate error of a factor of $\sqrt{2}$ in the final part of the corresponding expression in Ref. 6) for the relative amounts of t_1 noise to be expected for this simple model of pure phase irreproducibility in P-type gCOSY, N-type gCOSY and P- and N-type phase cycled COSY, respectively.

This calculation gives the relative t_1 noise levels for pure phase irreproducibility with random and uncorrelated phase errors, and assumes perfect 90° pulses, no relaxation and perfect field homogeneity. In the phase-cycled case, imperfect pulses and/or spin–lattice relaxation during t_1 would lead to further t_1 noise contributions from the axial peak coherence transfer pathway; this will also be the case in gCOSY if the gradient pulse areas are insufficient to suppress undesired pathways completely. In practice there will be errors in signal amplitude, pulse flip angle, frequency, lineshape, etc., as well as errors in phase; also, the frequency spectrum of the phase errors will not be white, i.e. the pulse phase errors will not be totally uncorrelated. Errors in amplitude and lineshape will affect all four types of experiment equally, while errors in frequency during t_1 should appear like phase errors and show similar differential effects, but will appear as frequency errors in t_2 and affect the four experiments similarly. Thus a real experiment is likely to show behaviour somewhere in between the two extremes of equal t_1 noise in all four experiments, as seen for pure amplitude irreproducibility, and the ratio $1:\sqrt{5}:\geqslant\sqrt{6}$ seen for pure phase irreproducibility. A comparison between the experimental ratios and these two limits could in principle give some information on the types of perturbation causing t_1 noise; another potential source for such information might be the asymmetry of the t_1 noise pattern about the f_1 frequencies of signals, since amplitude modulation of the t_1 signal should result in a modulation pattern which is symmetric.

EXPERIMENTAL

500 MHz proton absolute value COSY experiments were carried out on a sample of the tetracyclic orthoamide **1** in deuterioacetone, using a 5 mm triple resonance pulsed field gradient probe on a Varian Unity 500 spectrometer, slightly modified[7] to improve

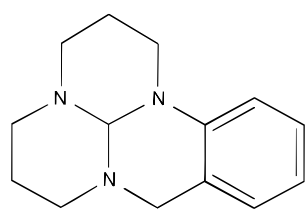

1

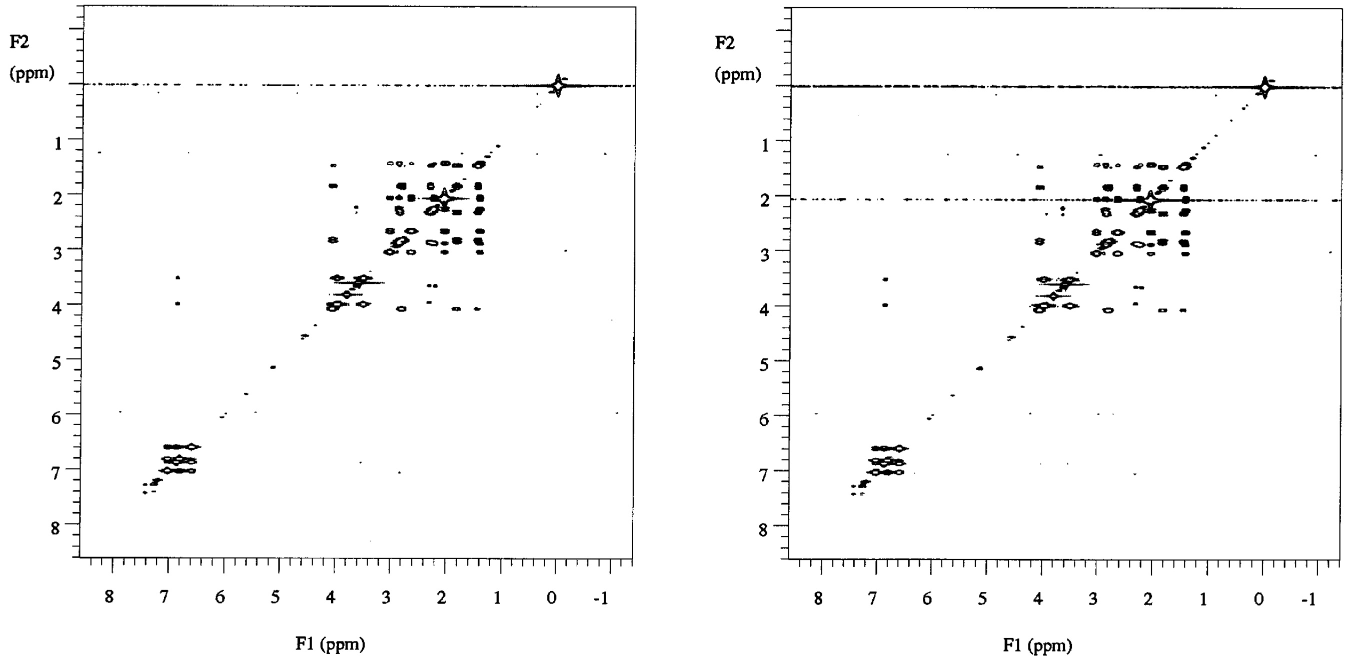

Figure 2. Absolute value mode 500 MHz proton gradient COSY spectra of **1**, measured using (left) the P-type and (right) the N-type versions of the sequence in Fig. 1.

stability; 256 increments of 2048 complex data points were measured using a long recycle time of 15.4 s, with f_1 and f_2 spectral widths of 5000 Hz. Gradient COSY experiments were carried out using a single transient per increment, with rectangular gradient pulses of 2.0 ms duration and approximtely 3 G cm^{-1} strength. Phase-cycled data were obtained using the split phase cycling conventionally used for hypercomplex phase sensitive COSY,[8] with four transients per increment, and recombined with appropriate signs to give N- and P-type datasets corresponding to eight transients per increment. Data were processed with one zero-filling in t_1 and sine-bell weighting centred on 0.026 s in t_1 and 0.102 s in t_2.

RESULTS

Figure 2 shows a comparison between the full absolute value gCOSY spectra obtained using P- and N-type gradient signs. The difference in t_1 noise between the two experiments can be seen more clearly in Fig. 3, which compares expansions of, and cross-sections through, the region of the gCOSY spectrum around the signal of tetramethylsilane (TMS). Figures 4 and 5 similarly compare the P- and N-type phase cycled data. All four figures use the same horizontal, vertical and intensity scales for display. The phase-cycled data clearly show the presence of coherent f_1 artefacts arising from the persistence of the modulation of longitudinal magnetization from increment to increment,[9] despite the relatively long recycle time; these artefacts are strongly attenuated by diffusion in gradient-enhanced experiments.

Peak heights and ratios of peak signal to root mean square noise were calculated for absolute value f_1 cross-sections in the 2D spectra, using the region between 6 and 7 ppm from TMS for the noise samples. The results are shown in Table 1, together with the relative ratios of noise to signal calculated with respect to the value for the P-type gradient COSY data; the noise-to-signal ratios for the phase cycled data were adjusted by a factor of $\sqrt{8}$ to allow for the greater number of transients measured. The figures in Table 1 show the influence of the effects discussed above, but are complicated by the differences in the lineshapes obtained in the two frequency domains with P- and N-type data, which result in a small but significant advantage in peak height for the N-type pathway because of the refocusing of static field inhomogeneity. This difference in peak

Table 1. TMS peak heights, signal to t_1 noise ratios and relative t_1 noise to signal ratios (adjusted for the effects of signal averaging) for f_1 cross-sections through absolute value mode COSY spectra

Parameter	P-type gradient	N-type gradient	P-type phase-cycled	N-type phase-cycled
TMS peak height (arbitrary units)	339	404	675	779
Signal to noise ratio	1927	1318	3444	3688
t_1 Noise relative to P-type gradient COSY	1	1.74	3.15	3.39

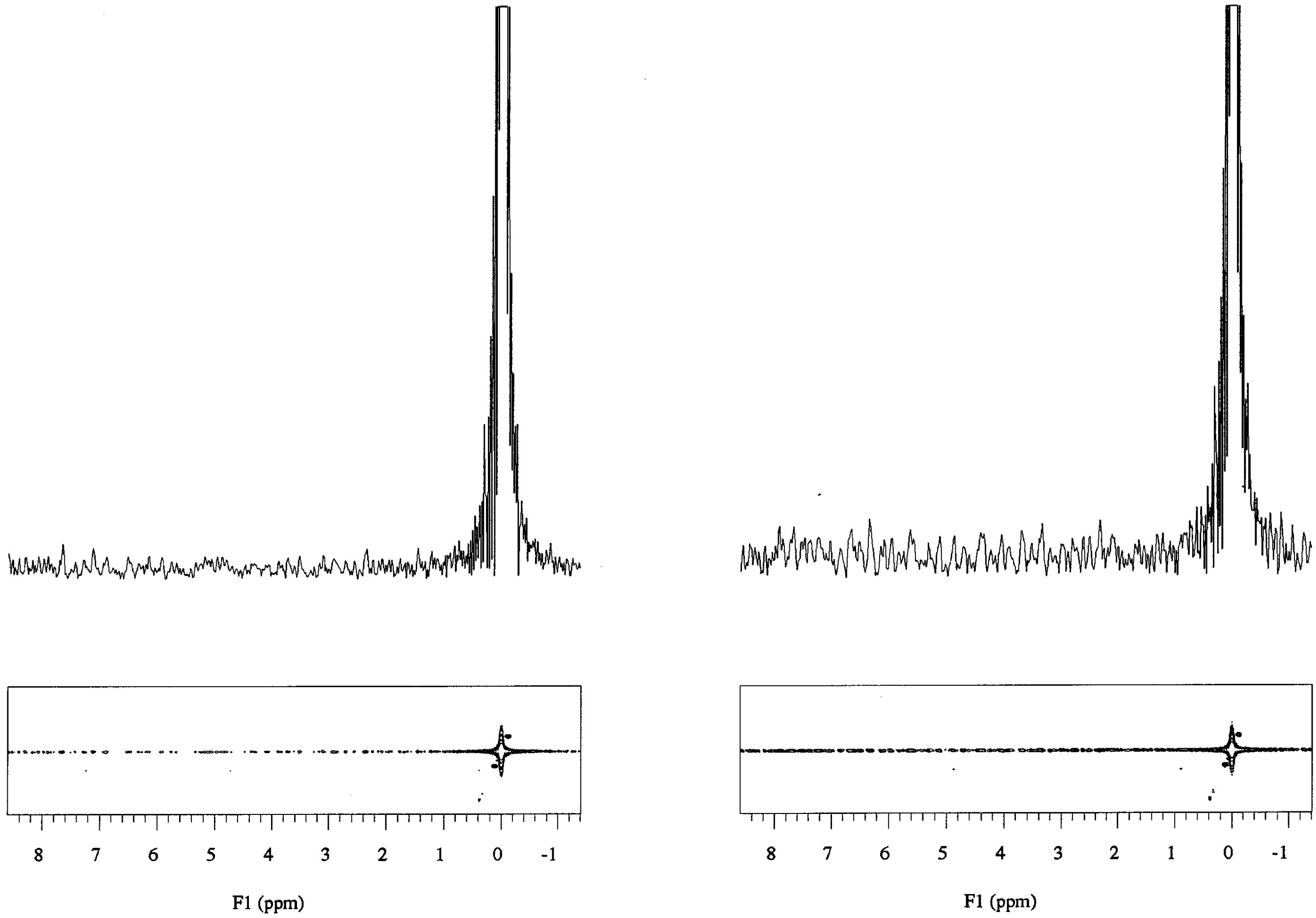

Figure 3. Expansions of (bottom) and cross-sections through (top) the P-type (left) and N-type (right) spectra in Fig. 2, centred on the TMS signal.

height reflects the different signal envelopes in t_1: the N-type envelope rises, because in the absence of significant relaxation the signal maximum in each free induction decay moves to longer times as t_1 is incremented, while the P-type t_1 envelope decays. The bias that this introduces in the data in Table 1 can be reduced by comparing the ratios of integrated f_1 noise power to integrated f_1 signal power in cross-sections through the

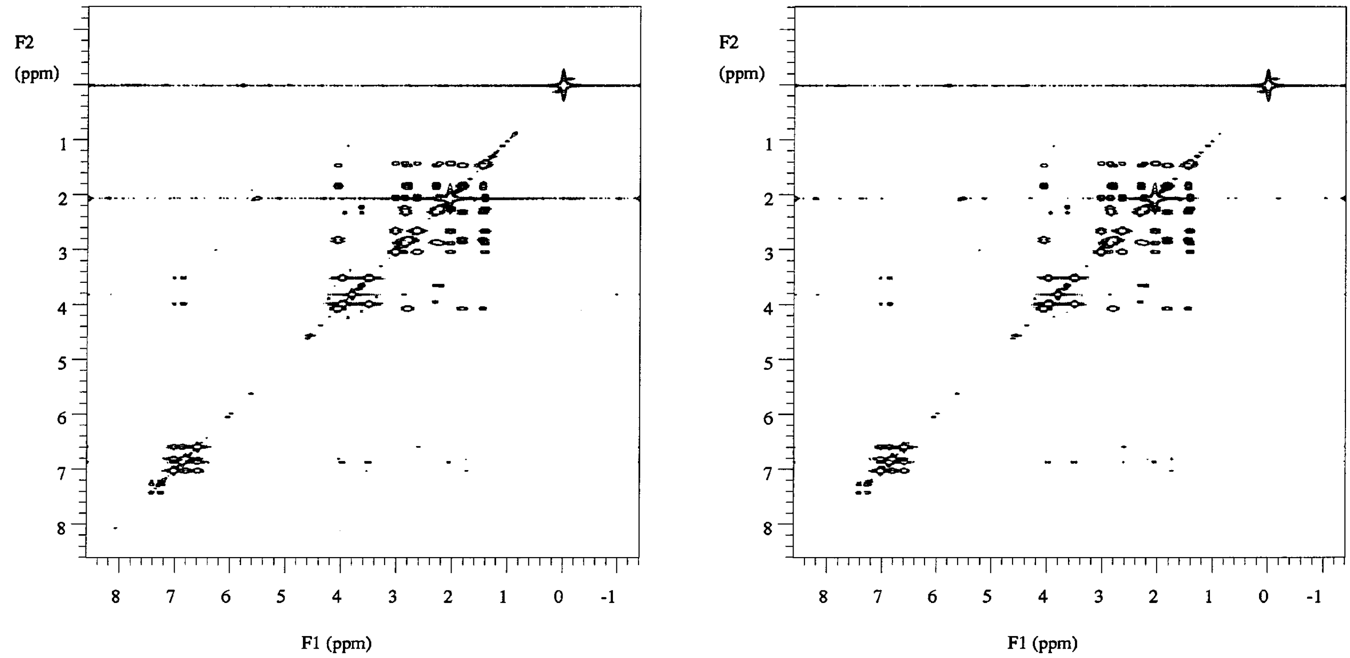

Figure 4. Absolute value mode phase-cycled COSY spectra of **1**, measured using the phase-cycled version of the sequence in Fig. 1 with the two experimental data sets combined to give (left) P-type and (right) N-type coherence transfer.

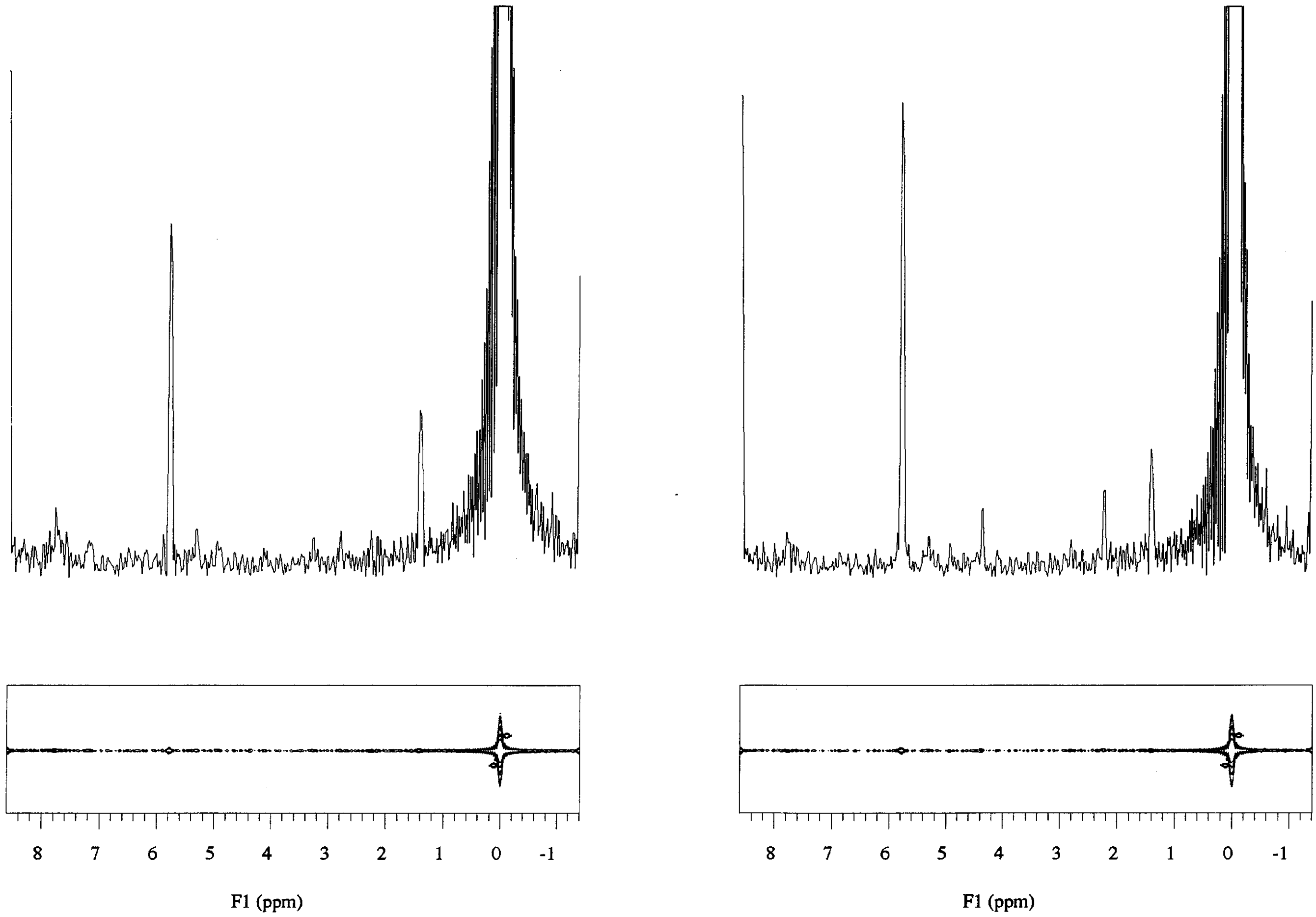

Figure 5. Expansions of (bottom) and cross-sections through (top) the P-type (left) and N-type (right) spectra in Fig. 4, centred on the TMS signal, as in Fig. 3.

spectra; these quantities can be found conveniently by integration of the power mode spectra. Integrated noise powers and signal powers for f_1 cross-sections through the TMS signal are shown in Table 2; once again the noise was determined for the region 6–7 ppm, and the power noise levels for the phase-cycled data were scaled up by a factor of 8 to allow for the effects of averaging.

DISCUSSION

It is sometimes asserted that gradient-enhanced experiments do not show t_1 noise. As the analysis above and the experimental results quoted show, this is not the case; indeed, t_1 noise levels in phase-cycled COSY are only a little worse than in N-type gradient COSY. (Gradient enhanced methods do, however, enjoy much lower levels of rapid pulsing artefacts, largely because of the effects of diffusion.) The qualitative conclusions that ratios of signal to t_1 noise are higher in P-type gradient COSY than in N-type, and that P-type gradient COSY shows significantly less t_1 noise than either phase-cycled COSY experiment, are supported by the data in Table 1, which show relative t_1 noise-to-signal ratios of 1:1.74:3.15:3.39 for P-type gradient COSY, N-type gradient COSY, P-type phase cycled COSY and N-type phase-cycled COSY, respectively, compared with the predicted ratios of 1:2.24:2.45:2.45.

Table 2. Integrated TMS signal power, t_1 noise powers and relative ratios of t_1 noise power to signal power (adjusted for the effects of signal averaging) for f_1 cross-sections through power mode COSY spectra

Parameter	P-type gradient	N-type gradient	P-type phase-cycled	N-type phase-cycled
TMS signal power (arbitrary units)	1759	2502	9307	6989
t_1 Noise power (arbitrary units)	0.0125	0.0594	0.0263	0.0200
t_1 Noise power/signal power relative to P-type gradient COSY	1	3.34	3.18	3.22

The data in Table 1 are skewed by the lineshape differences between P- and N-type experiments, so the data in Table 2 offer a better guide to the true t_1 noise levels. Here the t_1 noise powers for the four experiments are in the ratio 1:3.34:3.18:3.22, compared with the theoretical values for pure phase irreproducibility of 1:5:6:6, suggesting that there is some t_1 noise from sources other than phase irreproducibility, but that t_1 noise from the axial peak coherence transfer pathway in the phase-cycled experiments is not significant. The figures reported for the t_1 noise in Tables 1 and 2 have significant uncertainties, because of the relatively small samples of noise available, and also show a dependence on the time-domain weighting functions used. The t_1 noise advantages of P-type over N-type gradient COSY, however, remain clear over a wide range of different processing conditions. The reduction in the apparent advantage in t_1 noise-to-signal ratio enjoyed by gradient over phase-cycled COSY when the ratio of integrated noise power to signal power is computed as in Table 2, rather than the ratio of root mean square absolute value noise to signal peak height as in Table 1, is interesting; it may simply reflect the small systematic contribution made to the noise power figures in Table 2 by the tail of the TMS signal lineshape in f_1.

The practical implications of the results presented here become significant in cases where signals are sufficiently strong that the limiting factor in detection of cross peaks is t_1 noise rather than thermal noise. In a well designed modern high-resolution spectrometer this may not be until the signal to thermal noise ratio is over 1000:1, but in situations such as *in vivo* spectroscopy where stability is much more difficult to achieve the P-type experiment may prove advantageous with comparatively modest signal strengths. The t_1 noise advantage of P-type gCOSY over N-type arises because the P-type pathway in gCOSY confers immunity to changes in the phase of the mixing pulse, but the advantage will not necessarily extend to P-type pathways in other pulse sequences. For example, in gradient-enhanced NOESY the mixing period contains two 90° pulses bracketing the mixing delay, so that although the P-type pathway shows no net change in coherence order over the mixing period, the two pulses produce equal and opposite coherence order changes of one unit. Each pulse contributes its own phase error to the cumulative total over the sequence, and so the P-type pathway will only show a t_1 noise advantage over the N-type to the extent that the phase errors in the two pulses are correlated.

Acknowledgements

This work was supported by grants from the EPSRC (grants GR/H59251 and GR/K16296). G.A.M. thanks the Leverhulme Trust for a Research Fellowship. The sample of **1** was kindly provided by Dr J. A. Joule.

REFERENCES

1. K. Nagayama, A. Kumar and R. R. Ernst, *Biochem. Biophys. Res. Commun.* **90**, 305 (1979).
2. A. Bax, R. Freeman and G. A. Morris, *J. Magn. Reson.* **42**, 164 (1981).
3. R. E. Hurd, *J. Magn. Reson.* **87**, 422 (1990).
4. G. A. Morris, *J. Magn. Reson.* **80**, 547 (1988).
5. A. Gibbs, G. A. Morris, A. G. Swanson and D. Cowburn, *J. Magn. Reson. A* **101**, 351 (1993).
6. T. J. Horne and G. A. Morris, *J. Magn. Reson. A* **123**, 246 (1996).
7. G. A. Morris, *J. Magn. Reson.* **100**, 316 (1992).
8. D. J. States, R. A. Haberkorn and D. J. Ruben, *J. Magn. Reson.* **48**, 286 (1982).
9. N. Murali and A. Kumar, *Chem. Phys. Lett.* **128**, 58 (1986).